ScienSage

Journal of Advanced Scientific Research

Available online through http://www.sciensage.info

ISSN
0976-9595
Short Communication

SPECTROSCOPIC, MESP AND HIRSHFELD SURFACE ANALYSIS ON TYRAMINE ALKALOID BY DENSITY FUNCTIONAL THEORY METHODS

J. Priscilla[1, 2], D. Arul Dhas[2]

[1]*Research Scholar, Register Number: 12097, Manonmaniam Sundaranar University, Abishekapatti, Tirunelveli, Tamil Nadu, India*

[2]*Department of Physics, Physics Research Centre, Nesamony Memorial Christian College, Marthandam, Kanyakumari District, Tamilnadu, India*

**Corresponding author: priscillamoljp@gmail.com*

ABSTRACT

In this study, the molecular, electronic and chemical properties of alkaloid compound tyramine (TYA) have been investigated. The optimized molecular structure and vibrational frequencies have been calculated using B3LYP functional with 6-311G(d,p) basis set. NBO analysis reveals that the stability and charge transfer interaction of the molecule. The MESP analysis describes electrophilic and nucleophilic attack of the molecule. Hirshfeld surfaces and 2D fingerprint plots estimate the intra and intermolecular charge transfer interactions of TYA.

Keywords: DFT, alkaloid, NBO, MESP, Hirshfeld surface

1. INTRODUCTION

Tyramine (TYA) is a phenylethylamine alkaloid that is obtained from the amino acid tyrosine [1-2]. It is one of the trace amine, which possess important physiological effects such as neurohormone moderator and stimulates smooth muscles. It plays the role of an excitatory neurotransmitter [3], antidepressant [4] and antihypertensive [5]. The molecular formula for TYA is $C_8H_{11}NO$. Tyramine consists of hydroxyphenyl ring and ethylamine side chain. In the present study, the efforts have been taken to investigate the complete description of the molecular structure, vibrational frequencies, natural bond orbital (NBO) analysis, molecular electrostatic potential (MESP) analysis and hirshfeld surface analysis of alkaloid compound tyramine. B3LYP method at 6-311G(d,p) basis set was used to optimize the molecular structure of the title compound. Hirshfeld surface analyses have been performed to analyze the nature of interactions present in the TYA.

2. THEORETICAL STUDIES

All the quantum chemical computations were performed using Gaussian 09 program package [6]. The geometry optimization and vibrational frequencies calculation were performed by DFT method with the three parameter hybrid functional B3LYP with 6-311G(d,p) basis set [7-8]. Stability and charge transfer interactions were analyzed by NBO 3.1 program [9]. ArgusLab 4.0.1 [10] software was used to obtain the molecular electrostatic potential diagram of the molecule. Hirshfeld surface analysis and 2D fingerprint plots were calculated using CRYSTAL EXPLORER 3.1 program [11].

3. RESULTS AND DISCUSSION

3.1. Geometry optimization

The geometrical parameters of TYA are listed in Table 1. The optimized molecular structure of TYA is shown in Figure 1.

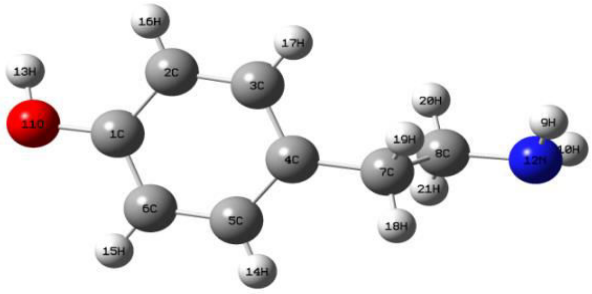

Fig. 1: Optimized structure of TYA

While comparing all C-C bonds in phenyl ring, the C_4-C_5 and C_3-C_4 bond lengths were elongated due to the attachment of ethylamine side chain. In phenyl ring, the C_6-H_{15} (1.083 Å) bond length was shortened due to the possibility of weak C_6-H_{15}…O_{11} hydrogen bonding interaction. Due to the influence of C_8-H_{20}…N_{12} hyperconjugative interaction, the C_8-H_{20} bond length increased while compared with other C-H bonds in ethyl

group. The bond angle value of phenyl ring shows that the ring is deviate from aromatic nature due to the substitution effect at C_1 and C_4 position. The dihedral angle value of phenyl ring is 0.0° which confirms the phenyl ring is in planar nature. But the dihedral angle of ethylamine group shows the nonplanar nature.

Table 1: Optimized parameters of TYA

Bond length (Å)	
C_1-C_2	1.394
C_2-C_3	1.394
C_3-C_4	1.397
C_4-C_5	1.401
C_5-C_6	1.391
C_6-C_1	1.395
C_6-H_{15}	1.083
O_{11}-H_{13}	0.963
C_8-H_{20}	1.101
C_8-H_{21}	1.094
Bond angle (°)	
C_1-C_2-C_3	119.8
C_2-C_3-C_4	121.5
C_3-C_4-C_5	117.6
C_4-C_5-C_6	121.7
C_5-C_6-C_1	119.7
C_6-C_1-C_2	119.7
Dihedral angle (°)	
C_1-C_2-C_3-C_4	0.0
C_4-C_5-C_6-C_1	0.0
H_{13}-O_{11}-C_1-C_2	0.1
C_3-C_4-C_7-C_8	-90.2
C_4-C_7-C_8-N_{12}	-178.2

3.2. Vibrational analysis

The vibrational frequencies with PED assignments are presented in Table 2. The calculated FTIR and FT-Raman spectra of TYA are shown in Fig. 2.

Table 2: Vibrational frequencies and their assignments of TYA

Calculated wavenumber (cm^{-1})		Assignments
unscaled	scaled	
3836	3630	OH stretching
3576	3399	NH_2 asymmetric stretching
3496	3327	NH_2 symmetric stretching
3191	3053	CH stretching
3164	3028	CH stretching
3158	3023	CH stretching
3145	3011	CH stretching
3071	2944	CH_2 asymmetric stretching
3048	2923	CH_2 asymmetric stretching
3015	2893	CH_2 symmetric stretching
2653	2561	CH_2 symmetric stretching
1658	1628	NH_2 scissoring
1654	1624	CC stretching
1630	1601	CC stretching
1543	1518	CH bending
1516	1492	CH_2 scissoring
1492	1469	CH_2 scissoring
1465	1443	CC stretching
1417	1397	CH_2 wagging
1358	1340	CH bending
1351	1333	CH_2 wagging
1345	1327	CC stretching
1318	1301	CH_2 wagging
1275	1260	CO stretching
1262	1247	CH_2 rocking
1226	1212	CC stretching
1194	1181	CH bending
1188	1175	OH bending
1154	1142	NH_2 rocking
1123	1112	CH bending
1076	1066	CN stretching
1041	1032	CH_2 twisting
1029	1021	CCC stretching
971	964	CH bending
963	956	CHCC wagging
933	927	CCCC puckering
861	856	CC stretching
840	836	CCHC wagging
828	824	NH_2 wagging
813	809	CH bending
788	785	CH_2 rocking
778	775	CC stretching
722	720	CCC stretching
656	655	CH bending
558	558	CCC deformation
512	512	CCC deformation
427	428	CH bending
421	422	CCOC torsion
382	383	CCCC torsion
328	329	CC twisting
313	314	CH_2 twisting
295	296	CO twisting
239	240	NH_2 twisting
201	202	CH_2 twisting
92	93	CNCC torsion
78	79	CCCC torsion
45	45	CCCC torsion

The OH stretching vibration is generally occurred in the around 3500 cm^{-1} [12]. The O_{11}-H_{13} stretching vibration is obtained at 3630 cm^{-1}. The increase in wavenumber

from the expected range is due to the influence of weak C_6-H_{15}...O_{11} hydrogen bonding interaction and steric effect between H_{13} and H_{16} (H_{13}...H_{16}=2.312 Å). Vibrational modes of 1,4-disubstituted phenyl ring analyzed on the basis of Wilson numbering scheme [13]. The mode 7b is expected in the range 3030-3050 cm^{-1}. The CH stretching vibration obtained at 3011 cm^{-1} is assigned to mode 7b. The CH_2 symmetric vibration obtained at 2945 and 2894 cm^{-1}. The CH_2 wagging and rocking mode lies at 1397, 1333 and 1247 cm^{-1}. The identification of CN stretching vibration is very difficult task due to several band overlaps on this region. The CN stretching mode generally appear in the region 1020-1220 cm^{-1} [14]. The band at 1301cm^{-1} is assigned to C_8-N_{12} stretching vibration. The shift in wavenumber is due to C_8-H_{20}...N_{12} hyperconjugative interaction. For primary amines, the NH_2 stretching bands are observed in the range 3420-3500 cm^{-1} [15]. The NH_2 symmetric and asymmetric stretching bands obtained at 3327 and 3399 cm^{-1} respectively.

3.3. NBO analysis

NBO analysis predicts the stability of the molecule based on the electron distribution in both filled and unfilled orbital. The second order perturbation theory analysis and hyperconjugative interactions of TYA are listed in Table 3.

The molecule TYA stabilized due to the orbital overlap of bonding $\sigma(H_{13}$-$O_{11})$ to antibonding $\sigma^*(C_1$-$C_6)$ show high stabilization energy (17.740 kJ/mol), which indicate electron delocalization occur within the molecule. The strong hyperconjugative interaction present C_8-H_{20} from N_{12} in TYA with stabilization energy 30.669 kJ/mol.

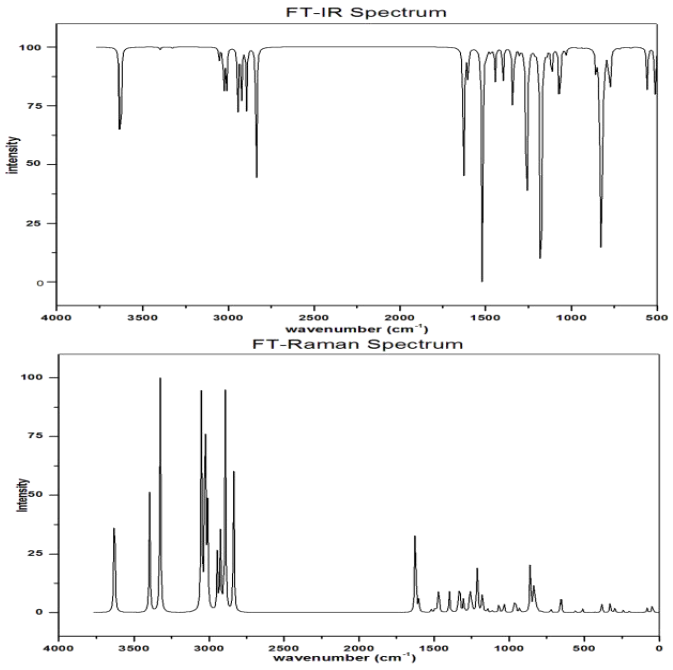

Fig. 2: FT-IR and FT-Raman spectrum of TYA

Table 3: Second order perturbation theory of Fock Matrix in NBO basis for TYA

DONOR NBO (i)	Electron Density (e)	ACCEPTOR NBO (j)	Electron Density (e)	$E^{(2)}$ kJ/mol
$\sigma(C_2$-$C_3)$	1.974 -0.699	$\sigma^*(C_4$-$C_7)$	0.020 0.433	14.937
$\sigma(C_5$-$C_6)$	1.699 -0.251	$\sigma^*(C_1$-$C_{11})$	0.025 0.343	15.983
$\sigma(C_4$-$C_7)$	1.975 -0.617	$\sigma^*(C_8$-$C_{12})$	0.009 0.355	7.699
$\sigma(C_7$-$C_8)$	1.975 -0.595	$\sigma^*(C_3$-$C_4)$	0.024 0.585	10.920
$\sigma(H_{13}$-$O_{11})$	1.987 -0.745	$\sigma^*(C_1$-$C_6)$	0.025 0.565	17.740
$n_1(N_{12})$	1.959 -0.310	$\sigma^*(C_8$-$H_{20})$	0.032 0.389	30.669
$n_1(N_{12})$	1.959 -0.310	$\sigma^*(C_8$-$H_{21})$	0.018 0.400	4.895

3.4. MESP analysis

The molecular electrostatic potential (MESP) map predicts the reactive site of nucleophilic and electrophilic attack for the TYA molecule. MESP plot of TYA is displayed in figure 3. In colour coding scheme, the red represents the most electronegative i.e, electron

rich area and white corresponds to electropositive centre i.e, electron poor area. It is noticeable that the electronegative region was located over the oxygen (O_{11}) and nitrogen (N_{12}) atoms in the molecule which effectively act as electrophilic attack. The electropositive region was located over the hydrogen atoms in the molecule which effectively acts as nucleophilic attack.

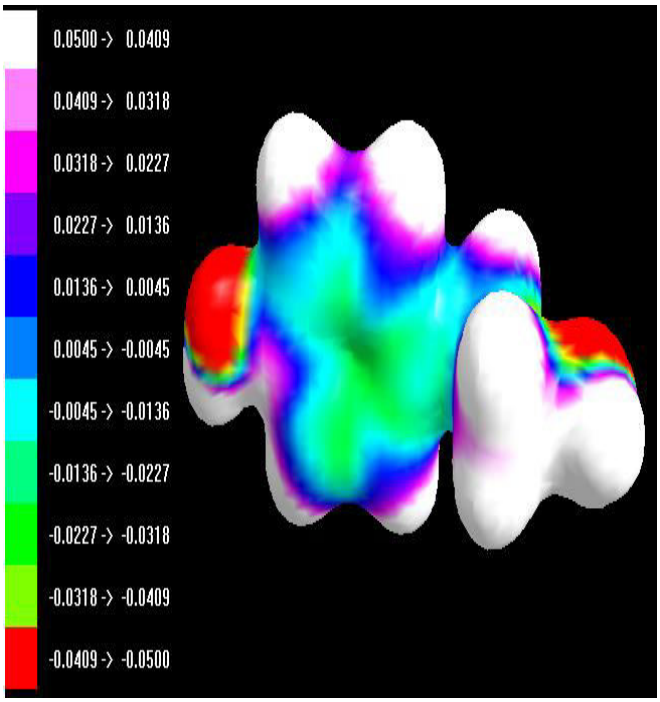

Fig. 3: MESP diagram of TYA

3.5. Hirshfeld surface analysis

Hirshfeld surface analysis predicts the surface characteristics of the molecule[16]. The hirshfeld surface (dnorm, de, di, curvedness and shape index) of TYA is shown in figure 4. The normalized contact distance (dnorm) based on red, white and blue colour scheme, which indicates closer contact, Van der Walls contact and longer contact respectively. The red spots on the surface of TYA in dnorm correspond to the nitrogen and oxygen atoms interact hydrogen bond with neighbouring molecules. The curvedness is a measure of how much shape there is present in the molecule. The shape index indicate that the red concave region on the surface around the acceptor atom and blue region around the donor hydrogen atom. 2D fingerprint plots of TYA are shown in figure 5. The 2D fingerprint plot describes the close contact of particular atom pair in the molecule. The H…H contacts are the most dominant interactions in the TYA molecule with 60% contribution. The C…H contacts (23%) are the second dominant interactions due to the presence of C-H…π interactions in the molecule. The contribution of O…H contact is 12%. The N…H contacts account for 4.7% shows sharp outer spikes in the fingerprint plot.

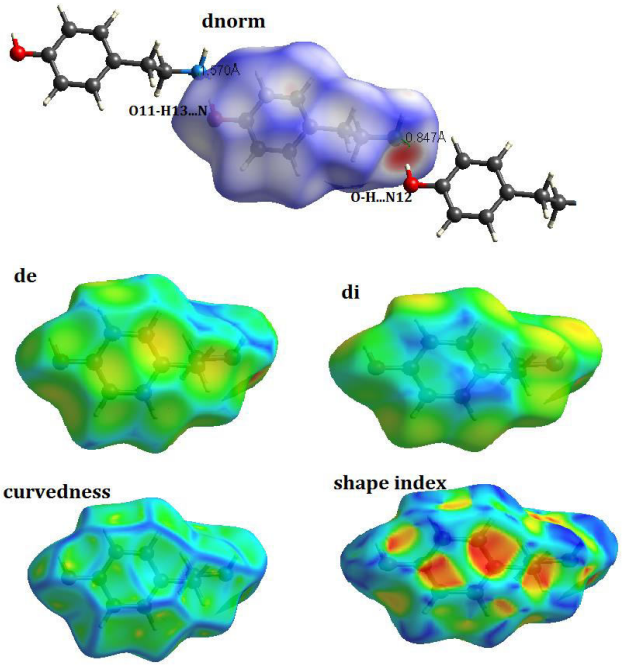

Fig. 4: Hirshfeld surfaces of TYA

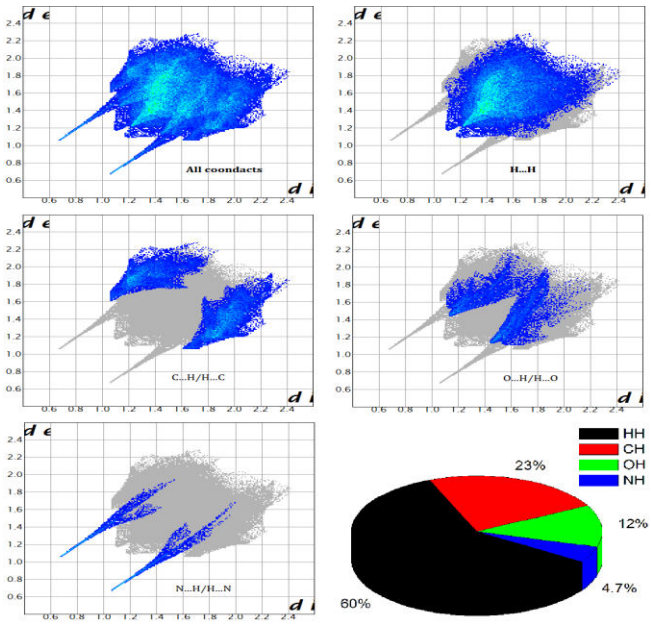

Fig. 5: 2D finger print plot and % of various intermolecular contacts contributed to the hirshfeld surface in the TYA compound

4. CONCLUSION

In the present work, the optimized geometry and vibrational wavenumbers of the alkaloid compound tyramine were determined and analyzed at DFT level of theory utilizing 6-311G(d,p) basis set. NBO analysis shows that the intramolecular hyperconjugative interaction between $n_1(N_{12}) \rightarrow \sigma^*(C_8\text{-}H_{20})$ bond orbitals. In MESP analysis the region around the O_{11} and N_{12} atoms shows negative potential and the hydrogen atom show positive potential. Hirshfeld surface analysis for H…H interaction of TYA exhibits 60% contribution.

5. REFERENCES

1. Rodolfo Quevedo, Nelson Nunez-Dallos, Klaus Wurst, Alvaro Duarte-Ruiz. *J. of Mol. Struc.,* 2012; **1029:**175-179.
2. Richardson P R, Bates S P, Jones A.C. *J. Phys. Chemistry A*, 2004; **108:**1233-1241.
3. Yadav T, Mukherjee V. *J. of Mol. Struc.*, 2017; **1147:**702-713.
4. Lulinski P, Sobiech M, Zolek T, Maciejewska D. *Talanta*, 2004; **129:**155-164.
5. Bianchetti M G, Minder I, Beretta-Piccoli C, Meier A, Weidmannu P. *Klinische Wochenschrift*, 1982; **60:**465-470.
6. Frisch M J, Trucks G W, Schlegel H B, Scuseria G E et al. Gaussian 09W Program, Gaussian Inc., Wallingford CT, 2009.
7. Becke AD. *J. Chem. Phys.*, 1993; **98:** 5648-5652.
8. Lee C, Yang W, Parr RG. *Phy. Rev.*, 1988; **37:**785-789.
9. Glendening DE, Reed AE, Carpenter JE, Weinhold F. NBO Version 3.1, TCI, University of Wisconsin, Madison, 1998.
10. Thompson MA. ArgusLab 4.0.1. Planaria software LLC, Seattle, WA, 2004.
11. Wolff SK, Grim Wood DJ, Mac Klmon JJ, Turner MJ, Jayathilaka D, Spackman AM. Crystal Explorer Vers. 3.1, 2017.
12. Smith B C. Infrared Spectral Interpretation: A Systematic Approach, CRC, Washington, DC, 1999.
13. Varsanyi G. Vibrational Spectra of Benzene Derivatives, Academic Press, New York, 1969.
14. Brian Smith C. Infrared spectral interpretation a systematic approach, CRC Press, NewYork, 1999.
15. George Socrates. Infrared and Raman characteristic group frequencies, John Willey and Sons Ltd, 2001.
16. Shamsuzzaman, Hena Khanam, Ashraf Mashrai, Mohd Asif, Abad Ali,Assem Barakat, Yahia Mabkhot N. *Journal of Taibah University for Science*, 2017; 11: 141-150.